EUKARYOTIC CELL, Dec. 2006, p. 2014–2023 Vol. 5, No. 12
1535-9778/06/$08.00+0 doi:10.1128/EC.00146-06

Activity of a Second *Trypanosoma brucei* Hexokinase Is Controlled by an 18-Amino-Acid C-Terminal Tail▽

Meredith T. Morris,[1] Courtney DeBruin,[1] Zhaoqing Yang,[2] Jeremy W. Chambers,[1] Kerry S. Smith,[1] and James C. Morris[1]*

Department of Genetics and Biochemistry, Clemson University, Clemson, South Carolina 29634,[1] and Department of Parasitology, Kunming Medical College, Kunming, Yunnan, People's Republic of China 650031[2]

Received 19 May 2006/Accepted 7 September 2006

Trypanosoma brucei **expresses two hexokinases that are 98% identical, namely, TbHK1 and TbHK2. Homozygous null TbHK2$^{-/-}$ procyclic-form parasites exhibit an increased doubling time, a change in cell morphology, and, surprisingly, a twofold increase in cellular hexokinase activity. Recombinant TbHK1 enzymatic activity is similar to that of other hexokinases, with apparent K_m values for glucose and ATP of 0.09 ± 0.02 mM and 0.28 ± 0.1 mM, respectively. The k_{cat} value for TbHK1 is 2.9×10^4 min^{-1}. TbHK1 can use mannose, fructose, 2-deoxyglucose, and glucosamine as substrates. In addition, TbHK1 is inhibited by fatty acids, with lauric, myristic, and palmitic acids being the most potent (with 50% inhibitory concentrations of 75.8, 78.4, and 62.4 μM, respectively). In contrast to TbHK1, recombinant TbHK2 lacks detectable enzymatic activity. Seven of the 10 amino acid differences between TbHK1 and TbHK2 lie within the C-terminal 18 amino acids of the polypeptides. Modeling of the proteins maps the C-terminal tails near the interdomain cleft of the enzyme that participates in the conformational change of the enzyme upon substrate binding. Replacing the last 18 amino acids of TbHK2 with the corresponding residues of TbHK1 yields an active recombinant protein with kinetic properties similar to those of TbHK1. Conversely, replacing the C-terminal tail of TbHK1 with the TbHK2 tail inactivates the enzyme. These findings suggest that the C-terminal tail of TbHK1 is important for hexokinase activity. The altered C-terminal tail of TbHK2, along with the phenotype of the knockout parasites, suggests a distinct function for the protein.**

The unicellular eukaryote *Trypanosoma brucei* is the causative agent of human African trypanosomiasis and nagana, an important livestock disease. Glycolysis is intimately linked to parasite survival in several ways. In mammals, bloodstream-form (BSF) parasites rely exclusively on glycolysis for energy. Glycolysis is also important to the biology of insect-stage (procyclic-form [PF]) parasites. RNA interference of glycolysis genes triggers a change in surface molecule expression. Because these molecules are found at the interface of the parasite and host, regulation of expression of surface molecules is likely very important (18). Furthermore, rapid inhibition of glycolysis in PF parasites, either through specific inhibitors of the pathway or through RNA interference silencing of some enzymes within the pathway, can be lethal (5, 18).

Hexokinase (HK), the first enzyme of the glycolytic and pentose phosphate pathways, catalyzes transfer of the γ-phosphoryl group of ATP to glucose, yielding glucose-6-phosphate (G6-P). Early studies of *T. brucei* hexokinase activity revealed that the enzyme activity was unconventional. While other characterized HKs exist as monomers or dimers, *T. brucei* HK forms multimers containing up to six subunits (15). Additionally, unlike most HKs from other eukaryotes, *T. brucei* HK is not inhibited by G6-P (its product) and can utilize ITP, UTP, CTP, and GTP, in addition to ATP, as substrates (15, 19).

The completion of the *T. brucei* genome project (strain TREU927/4 GUTat10.1) revealed the presence of two hexokinase genes, namely, Tb*HK1* and Tb*HK2*, in tandem on chromosome 10. These genes encode polypeptides that are 98% identical, and transcripts for both genes have been identified in PF parasites (18). Recently, proteomic analysis of purified glycosomes revealed that both proteins are present in the PF and BSF parasite life stages (4).

Because TbHK1 and -2 are 98% identical, are expressed in the same life stages (4), and may form multimers of unknown ratios of TbHK1 and -2, studying the distinct roles of these two proteins in the parasite has proven challenging. Here we present a phenotypic analysis of TbHK2-knockout parasites, and we demonstrate that the two nearly identical proteins have very different biochemical properties in vitro.

MATERIALS AND METHODS

Trypanosome growth and transformation. PF *T. brucei* 29-13, a 427 strain that expresses T7 RNA polymerase and a tetracycline repressor, was grown in SDM-79 supplemented with 10% heat-inactivated fetal bovine serum as described previously (27, 30). This strain was used as the parental strain throughout this work. SDM-80 without glucose was prepared as described previously (13) and supplemented with 9% heat-inactivated dialyzed serum (Sigma) and 1% heat-inactivated serum. Parasite growth was monitored on a Becton Dickinson FACScan flow cytometer. Transfections and selections for stable integration were performed as described previously (26).

Generation of TbHK2 knockout PF parasites. To knock out single alleles of the Tb*HK2* gene, parasites were transfected with PCR-generated linearized DNA constructs carrying the blasticidin resistance gene (*bsr*) flanked by the 5′ and 3′ untranslated regions (UTRs) of the targeted gene (see Fig. 2A). To generate the construct used to knock out the first allele of Tb*HK2*, a forward primer (primer 1 [TGTTTATGCTGCTGCTTTGC]) was paired with the fusion primer TbHK2-131Bla1-22 (CTTGAGACAAAGGCTTGGCCATTATCGATC CACACGGCAGTA [contains the first 22 nucleotides {nt} of the *bsr* gene fused

* Corresponding author. Mailing address: Department of Genetics and Biochemistry, Clemson University, 214 Biosystems Research Complex, 51 New Cherry Street, Clemson, SC 29634. Phone: (864) 656-0293. Fax: (864) 656-0393. E-mail: jmorri2@clemson.edu.

▽ Published ahead of print on 6 October 2006.

to 20 nt from position −40 of the TbHK2 5′ UTR]) in a PCR with *T. brucei* genomic DNA as the template to yield the forward long primer (TbHK2FLP). The reverse long primer (TbHK2RLP) was generated by PCR, using a fusion primer (Bla.371TbHK2.1617 [GGTTATGTGTGGGAGGGCTAAAGCGACT TTTGCATTTCGTT]) containing the last 21 nt of the *bsr* gene fused to the sequence at position +1617 of the 3′ UTR of Tb*HK2* in combination with a reverse primer (primer 2 [CTGTTTTCGTCGATGCAAAATTTTGCATCGAC GAAAACAG]) containing the sequence from position +1790 of the 3′ UTR of Tb*HK2*. TbHK2FLP and TbHK2RLP were then used as primers in a PCR with the *bsr* gene as the template, from which the full-length *bsr* knockout construct was further enriched by PCR. The PCR products were cloned into pGEM-T Easy (Promega, Madison, Wisconsin) and used in PCRs to generate linear DNAs for transfection.

To target the second allele of Tb*HK2*, a modified approach was used, employing a three-step ligation to generate a fusion of the UTRs of Tb*HK2* flanking the puromycin resistance gene (*pur*) (see Fig. 2A). First, *pur* was cloned by PCR into the pGEM-T Easy vector, with BamHI and HindIII sites added to *pur* using primers Fpur1-21BamHI (GATCGGATCCATGACCGAGTACAAGACC) and Rpur601*Hind*III (GATCAAGCTTTCAGGCACCGGGCTTGCGGGTC), yielding pGEM:pur. The 5′ UTR of *HK2* was amplified from *T. brucei* genomic DNA, using primer FTbHK2.-322NcoI (GATCCCATGGTGTTTATGCTGCT GCTTTGC [with an NcoI site added to the 5′ end]) and primer RTbHK2.-131BamHI, which includes a BamHI site (GATCGGATCCTATCGATCCACA CGGCAGTA). The resulting amplicon was digested with BamHI and NcoI and ligated into similarly digested pGEM:pur to yield pGEM:HK2pur. The Tb*HK2* 3′ UTR was cloned downstream of the *pur* gene by a similar approach, using the forward primer FTbHK2.1617*Hind*III (GATCAAGCTTAGCGACTTTTGCAT TTCGTT) and the reverse primer RTbHK2.1790PstI (GATCCTGCAGTTTTG CATCGACGAAAACAG). The product was digested with HindIII and PstI and ligated into pGEM:HK2pur to generate pGEM:HK2purHK2. FTbHK2.-322NcoI and RTbHK2.1790PstI were used with pGEM:HK2purHK2 as a template to generate linear DNA for transfection.

Immunolocalization and Western blotting of TbHK2. To localize TbHK2, the full-length open reading frame (ORF) was cloned into pLew111(2T7)GFPβ (the generous gift of Shawn Motyka and Paul Englund, Johns Hopkins School of Medicine). This vector fuses green fluorescent protein (GFP) to the carboxyl termini of expressed proteins. Strain 29-13 PF trypanosomes were transformed with linearized DNA and selected as described above. Recombinant TbHK2 (rTbHK2) expression was induced in PF 29-13 cells harboring pLew111(2T7) TbHK2/GFP by the addition of tetracycline (1 μg/ml). Cells were allowed to adhere to poly-L-lysine-coated slides, fixed (4% paraformaldehyde, 5 min, room temperature [RT]), permeabilized (0.1% Triton X-100, 15 min, RT), and then washed twice (5 min) with phosphate-buffered saline supplemented with 0.1 M glycine. Cells were then stained with a mouse monoclonal antibody against the GFP tag (Rockland Immunochemicals, Gilbertsville, PA) and a rabbit anti-*T. brucei* glycosomal antibody (2841D) (21), raised primarily against the glycosomal proteins pyruvate phosphate dikinase, aldolase, and glyceraldehyde phosphate dehydrogenase (21) (the kind gift of Marilyn Parsons [Seattle Biomedical Research Institute, Seattle, WA]). Primary antibodies were detected with fluorescein isothiocyanate-conjugated goat anti-mouse or Texas Red-conjugated goat anti-rabbit (Rockland, Gilbertsville, PA) secondary antibodies.

Western blotting was performed on pellet fractions obtained by centrifugation at 17,000 × *g*, which were prepared as described previously (4). Briefly, parasites (5×10^8) were grown to log phase, harvested by centrifugation, washed, freeze-thawed, and lysed by grinding in silicon carbide. Following cell disruption, the lysate was centrifuged (100 × *g*, 15 min) to remove the abrasive, followed by a second centrifugation step (1,000 × *g*, 15 min) to remove the nuclei. The supernatant was centrifuged (17,000 × *g*, 15 min) to yield a 17,000 × *g* pellet (which contains glycosomes), which was solubilized in sodium dodecyl sulfate-polyacrylamide gel electrophoresis (SDS-PAGE) loading buffer, resolved by 10% SDS-PAGE, and transferred to a nitrocellulose support. The membrane was blocked with 1% nonfat milk in 1× TNT (10 mM Tris-Cl, pH 8.0, 150 mM NaCl, 0.05% Tween 20), and the primary antibody was applied. Blots were stained with anti-TbHK2 (αTbHK2; 1:20), an affinity-purified polyclonal antibody generated against a peptide (CGVGAALISAIVADGK) conjugated to keyhole limpet hemocyanin (Rockland Immunochemicals, Inc., Gilbertsville, PA), or αHxk597, a polyclonal antibody raised against *Arabidopsis* Hxk1 (1:2,500) (kindly provided by Brandon Moore, Clemson University), in blocking buffer for 1 h at RT. Following incubation with a horseradish peroxidase-conjugated secondary antibody (1:10,000, 1 h), the membranes were developed using SuperSignal West Pico chemiluminescent substrate (Pierce Biotechnology, Inc., Rockford, IL).

Northern blotting and hybridization. Total RNA was purified from parasites (Purescript RNA isolation kit; Gentra Systems), and 10 μg was electrophoresed in formaldehyde-1.5% agarose gels. rRNA levels were estimated by ethidium bromide staining to ensure that equal amounts of total RNA were loaded in all lanes. RNAs were then transferred to a GeneScreen Plus transfer membrane (NEN Life Science Products, Inc., Boston, MA). A TbHK1-specific ^{32}P-labeled probe was made by random priming of a 297-bp fragment of the TbHK1 gene (starting 1,388 bp downstream of the TbHK1 gene's initiating ATG), while the TbHK2-specific probe was generated using a 474-bp portion of the TbHK2 gene (starting 1,316 bp from the initiating ATG). Hybridization was carried out and blots were washed as described previously (18). The percent reductions in mRNA levels were estimated by densitometry of appropriately exposed autoradiograms.

Bacterial expression of recombinant TbHK1 and -2. Open reading frames of Tb*HK1* and *-2* lacking the initiating Met codon were amplified by PCR from genomic DNA isolated from PF 29-13 (427 strain) parasites and cloned into pQE30 (QIAGEN, Valencia, CA) in frame downstream of a six-His tagging sequence. Constructs were confirmed to be correct by sequencing. Plasmids were transformed into *Escherichia coli* M15(pREP), and cultures were grown to log phase and induced at 30°C overnight with 0.25 mM isopropyl-β-D-thiogalactopyranoside (IPTG). Soluble proteins were purified using nickel-affinity chromatography (20). Glucose was omitted from the purification procedure (without a detectable impact on enzyme activity) in order to assess the use of alternative hexoses as substrates. This method routinely yielded 30 μg/liter of purified soluble TbHK.

C-terminal domain swaps in TbHKs. To exchange the C-terminal tails of TbHK1 and TbHK2, pQE30 constructs harboring the Tb*HK1* and *-2* ORFs were digested with PstI, which cleaves at bp 988 of both ORFs and downstream of the ORF within the pQE30 multicloning site. The DNA fragment encoding the terminal 138 amino acids of each protein was gel purified and ligated to the 5′ portion of the other gene, yielding TbHK1 with the C terminus of TbHK2 (TbHK1C2) or TbHK2 with the C terminus of TbHK1 (TbHK2C1).

TbHK1 and -2 lacking the terminal 138 amino acids (TbHK1N and TbHK2N) were generated by PstI digestion of the pQE30 plasmid harboring the Tb*HK1* and *-2* ORFs, respectively. Vector lacking the 416-bp PstI insert was gel purified, and the gap was sealed by ligation. TbHKs lacking the last 18 amino acids (TbHK1C-18 and TbHK2C-18) were generated by PCR, using primers ForTbHK (AAGCTTGCGGCCGCTTATTGCGAGAACGGCCCTGAC) and RevTbHKN (GGATCCTCTAGACGCCTAAACAATATCC) in a reaction with pQE30 harboring either TbHK1 or -2 as the template.

Site-directed mutagenesis to yield TbHK1G93D and TbHK1S161A was performed using a QuickChange site-directed mutagenesis kit (Stratagene, La Jolla, California) and the following primers: FHK1.G93D, CGCACTTGACCTCGG TGATACCAACTTCCG; RHK1.G93D, CGGAAGTTGGTATCACCGAGGT CAAGTGCG; FHK1.S161A, GGGTTTACCTTCGCTTTCCCCGTGG; and RTbHK1.S161A, CCACGGGGAAAGCGAAGGTAAACCC. All constructs were cloned into pQE30 and verified by sequencing.

Hexokinase assays. Hexokinase assays were performed in triplicate, using a coupled reaction as described previously (16, 18). Briefly, assays used glucose-6-phosphate dehydrogenase (2 units/assay; EMD Biosciences, Inc., San Diego, CA) as a coupling enzyme to reduce NAD^+ to NADH during the oxidation of G6-P to 6-phosphogluconic acid. The final conditions were 0.1 M triethanolamine, pH 7.9, containing 1.0 mM ATP, 33 mM $MgCl_2$, 20 mM glucose, and 0.75 mM NAD^+ (2). Assays were performed in a 96-well microtiter plate format in a GENios spectrophotometer (Phenix Research Products, Hayward, CA). Kinetic values were determined using Lineweaver-Burke and Eadie-Hofstee analyses, with apparent K_ms determined using at least three experiments, with two separate enzyme preparations in each. The apparent K_m values for glucose, ATP, and UTP were determined by varying the concentration between 0.125 mM and 100 mM (glucose) or between 0.05 mM and 50 mM (ATP and UTP). To test inhibition by G6-P, an alternative coupled reaction was used. Pyruvate kinase (1 U; EMD Biosciences, Inc.) and lactate dehydrogenase (1 U) were included with HKs and inhibitors, along with 0.42 mM NADH and 25 mM phosphoenolpyruvate, and the depletion of NADH to NAD^+ was monitored spectrophotometrically at 340 nm. Fatty acid inhibition was performed by preincubation of HKs (60 min, 25°C) in 0.1 M Tris-acetate-EDTA, pH 7.9, supplemented with 12 mM $MgCl_2$, 1 mM dithiothreitol, 4 mM ATP, and various concentrations of fatty acids or equivalent volumes of the solvent used to solubilize the fatty acids. The incubation reaction was assayed for hexokinase activity as described above. As a control for all assays, *Saccharomyces cerevisiae* Hxk (a mixture of yeast Hxk1 and -2 at an unknown ratio; EMD Biosciences, Inc., San Diego, CA) was assayed in tandem with the TbHK experiments.

Modeling TbHKs. TbHK1, TbHK2, and TbHK1(N469D) were modeled on both the *Saccharomyces cerevisiae* HK structure (PDB accession no. 1IG8, GI accession no. 1150586) and the *Schistosoma mansoni* HK structure (PDB acces-

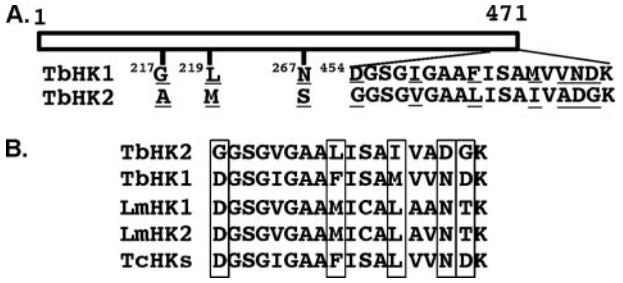

FIG. 1. (A) Comparison of TbHK2 and TbHK1 protein sequences. Amino acid differences are underlined. (B) Alignment of the C-terminal 18 residues of *T. brucei* (TbHK2 and TbHK1), *Leishmania major* (LmHK1 and LmHK2), and *T. cruzi* (TcHKs) HKs. The *L. major* sequences correspond to LmjF21.0240 and LmjF21.0250, while the single *T. cruzi* sequence is identical in both Tc00.1047053508951.20 and Tc00.1047053510121.20. Boxed residues are unique to TbHK2.

sion no. 1BDG, GI accession no. 5107491), using DS Modeler (Accelrys) with the standard parameters built into the program. The structures were visualized with DS Visualizer (Accelrys) and iMol (version 0.31). The *T. brucei* HK models were compared visually to the *S. cerevisiae* and *S. mansoni* HK structures to ensure that there were no major structural anomalies.

RESULTS

The *T. brucei* genome harbors two nearly identical HK genes in tandem on chromosome 10. Recently, peptides from both genes have been identified by mass spectrometry analysis of purified *T. brucei* glycosomes (4). While other organisms may have multiple highly similar hexokinases (those encoded by *Hxk1* and *-2* from yeast, for example), TbHK1 and -2 (GenBank accession no. AJ345044 and the *T. brucei* genome sequence corresponding to PDB accession no. XP_822457, respectively) are predicted to be much more similar to each other at the amino acid level (98% identical) than are the yeast enzymes (75% identical).

Predicted protein sequences for TbHK1 and -2 were compared with those of other hexokinases by using the Consurf algorithm (Consurf Server for the Identification of Functional Regions in Proteins, version 2.0 (Jul-02), available at http://consurf.tau.ac.il). First, the algorithm was used to generate a comparison of the 44 sequences of highest similarity to a model HK (yeast Hxk2), yielding a normalized conservation score for each residue. The TbHK1 and -2 sequences were then compared to the score and found to be highly similar (with the noted exception of the C-terminal six amino acids, which have been excluded from this comparison because they are completely distinct). TbHK1 and -2 share 61 of the 66 consensus amino acids found in all HKs analyzed, with the divergent residues being Asp^{78}, Lys^{80}, Ala^{82}, Thr^{141}, and Ile^{425}.

Although TbHK1 and TbHK2 are nearly identical, the majority of the differences (7 of the 10 total differences) between the two polypeptides are found in the divergent C termini of the proteins (Fig. 1). In some cases, the differences between TbHK1 and TbHK2 appear to be conserved, with hydrophobic residues substituted for hydrophobic residues (Ile^{458} and Val^{458}, for example). In other cases (Gly^{217} and Ala^{217}, Leu^{219} and Met^{219}, or Asn^{267} and Ser^{267}), Consurf analysis indicates that either amino acid alternative is found in other hexokinases. An 11th potential residue difference (Gly^{132} in TbHK1 to Asp^{132} in TbHK2, which results from a single nucleotide change) identified in the annotated *T. brucei* strain 927 genome database has not been detected in sequences using *T. brucei* strain 427 as the template. Additionally, this difference is not present in the annotated *T. brucei gambiense* HK1 and -2 sequences, suggesting that it may be a strain-specific polymorphism.

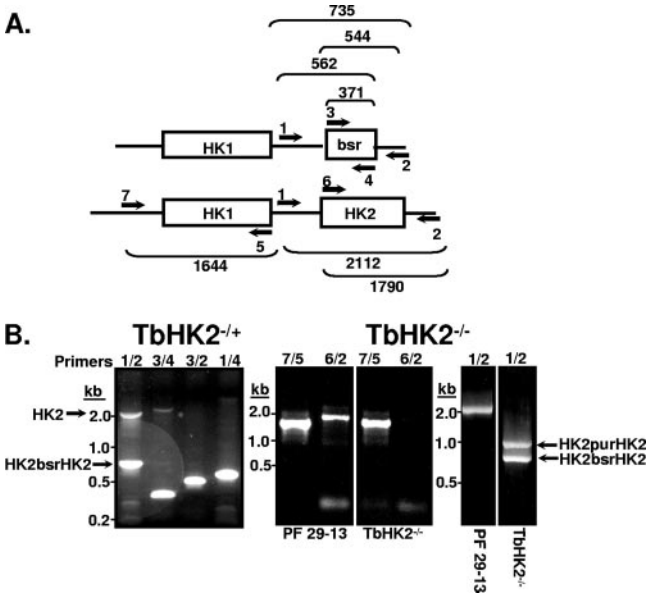

FIG. 2. Targeting TbHK2 for deletion. (A) Schematic representation of heterozygous null knockouts of TbHK2, with PCR product sizes indicated (not to scale). *bsr*, blasticidin resistance gene. (B) PCR analysis of genomic DNAs from a blasticidin-resistant single-allele knockout ($TbHK2^{-/+}$) and a blasticidin- and puromycin-resistant double-allele knockout ($TbHK2^{-/-}$).

TbHK2 gene ablation. Knockout of Tb*HK2* was initiated using a PCR-based approach to target the single-copy Tb*HK2* gene. This method generates a linear fragment of DNA that contains the blasticidin resistance gene (*bsr*) flanked by sequences from the targeted gene sufficient for efficient homologous recombination. We successfully generated single-allele Tb*HK2* knockouts ($TbHK2^{+/-}$), which we confirmed by PCR (Fig. 2B). PCR using primers for the Tb*HK2* UTRs (primers 1 and 2) in a reaction with genomic DNA from the blasticidin-resistant parasites yielded two products. The larger fragment (predicted to be 2,112 bp) corresponds to the intact authentic Tb*HK2* allele, while the smaller has the predicted size (735 bp) of *bsr* fused to the Tb*HK2* UTRs (Fig. 2B). Using primer sets consisting of a *bsr*-specific primer (either primer 3 or 4) and a UTR primer (primer 1 or 2) yielded products of the correct predicted size, indicating the presence of the integrated gene (Fig. 2B).

The $TbHK2^{+/-}$ cells were then used to generate double-allele knockouts. The blasticidin-resistant clone analyzed above was transformed with the *pur* gene fused to the UTRs of Tb*HK2*. Following the generation of parasites resistant to blasticidin and puromycin, the Tb*HK2* knockout was confirmed by PCR (Fig. 2B). Tb*HK1* was not altered in these parasites, as PCR using primers for the 5′ UTR of Tb*HK1* and the Tb*HK1* ORF yielded similar products whether parental 29-13 or

TbHK2$^{-/-}$ genomic DNA was used as the template in the reaction (Fig. 2A, primers 7 and 5). While parental 29-13 genomic DNA yielded a product with a primer set for the *HK2* ORF and *HK2* 3′ UTR (primers 6 and 2, predicted to result in a product of 1,790 bp), a similar reaction using TbHK2$^{-/-}$ genomic DNA was not fruitful (Fig. 2B). Conversely, PCR using PF 29-13 genomic DNA and antibiotic resistance gene-specific primers in combination with TbHK primers (or alone) did not yield a product. Using primers that flank the TbHK2 ORF (primers 1 and 2) yielded an ~2-kb PCR product when PF 29-13 genomic DNA was used as a template. A similar reaction using TbHK2$^{-/-}$ genomic DNA as the template (and primers 1 and 2) produced two products that corresponded in size to the *bsr* and *pur* genes inserted into the Tb*HK2* alleles (735 bp and 940 bp, respectively) (Fig. 2B). These products were cloned and sequenced, and the introduction of the drug resistance gene was confirmed. These observations have been supported by Southern blot analysis (not shown).

To score the impact of gene ablation on TbHK2 protein expression, we performed Western blotting using a polyclonal antibody specific to the C-terminal 15 residues of TbHK2 (αTbHK2). The affinity-purified αTbHK2 antibody reacts with recombinant TbHK2 but does not detect recombinant TbHK1, as the C-terminal 15 amino acids of the two proteins differ at six residues (Fig. 3A). TbHK2 expression in PF *T. brucei* was next explored by Western blotting of 17,000 × *g* pellet fractions from PF 29-13 and TbHK2$^{-/-}$ cells with αTbHK2. A single ~51-kDa protein band in the PF 29-13 sample reacted strongly with αTbHK2, while a similar fraction from TbHK2$^{-/-}$ cells lacked a detectable signal (Fig. 3B).

Cellular HK activity is increased in TbHK2$^{-/-}$ PF parasites. To determine if the knockout of TbHK2 led to a change in cellular HK activity, cell lysates of PF 29-13 and TbHK2$^{-/-}$ parasites were assayed in a coupled reaction for HK activity. Interestingly, HK activity was increased in the TbHK2$^{-/-}$ parasites (0.11 ± 0.001 U/mg) compared to that in parental cells (0.042 ± 0.003 U/mg) (Fig. 4A). A similar increase was noted if HK activity was assessed on a "per-cell" basis (Fig. 4B).

The increase in cellular HK activity corresponded to an increase in the TbHK1 protein level in the glycosome-enriched fraction, as determined by Western blotting of the 17,000 × *g* pellet, using a polyclonal antibody raised against *Arabidopsis* Hxk1 (αHxk597) which is specific to rTbHK1 (Fig. 3A). Probing the blot with αHxk597 revealed that TbHK1 was 4.48-fold more abundant in the TbHK2$^{-/-}$ sample (as determined by densitometry). To control for sample loading, the blot was also probed with α2841D, revealing that both glyceraldehyde-3-phosphate dehydrogenase and aldolase were 1.98-fold more abundant in the TbHK2$^{-/-}$ sample. When adjusted for loading, the net increase in the TbHK1 polypeptide (~2.5-fold) was in agreement with the increase in cellular HK activity observed in TbHK2$^{-/-}$ cells (Fig. 4). Interestingly, Northern blot analysis of parental and TbHK2 knockout cells using a probe specific for TbHK1 revealed an ~1.87-fold decrease in steady-state abundance of TbHK1 mRNA (Fig. 3C). Hybridizing the same blot with a probe specific for TbHK2 mRNA confirmed that the TbHK2 transcript was ablated in the TbHK2 knockout cells (Fig. 3C). These observations suggest that the increase in TbHK1 protein could be due to altered translation rates or changes in TbHK1 protein stability, even in the face of a decreased message.

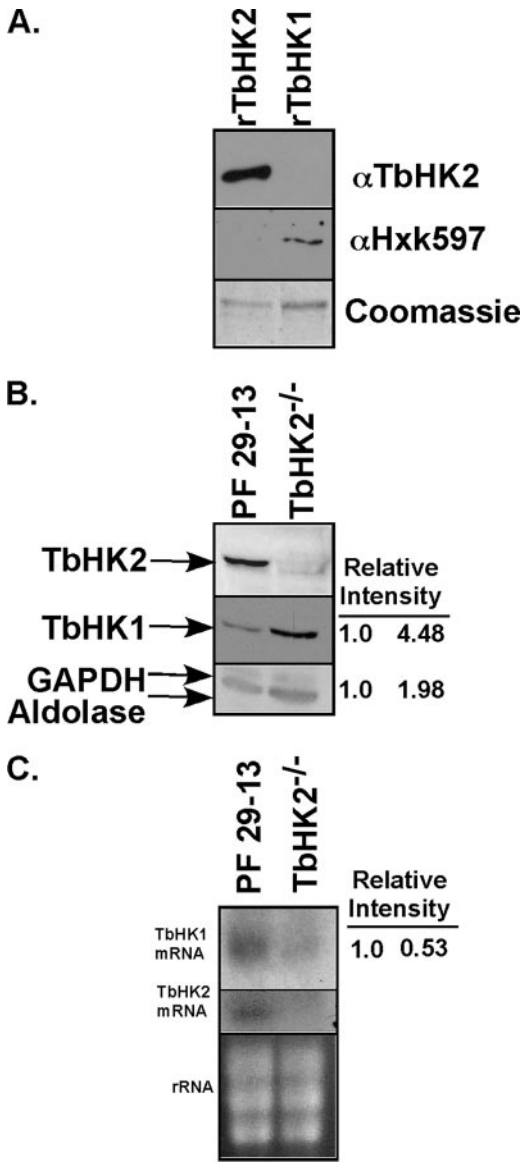

FIG. 3. Western and Northern blotting of TbHK2$^{-/-}$ cells. (A) Five hundred nanograms of recombinant TbHK2 and -1 (lanes 1 and 2) was resolved by SDS-PAGE, transferred to nitrocellulose, and probed with αTbHK2 and, after stripping of the blot, αHxk597. Peroxidase-conjugated secondary antibodies followed by chemiluminescence were used to visualize cross-reactive bands. A portion of a Coomassie-stained gel loaded with samples resolved by Western blotting is shown as a loading control. (B) Western blots of 17,000 × *g* pellet fractions from 1.5 × 10^8 PF 29-13 parental or TbHK2$^{-/-}$ parasites (lanes 1 and 2) probed with αTbHK2, αHxk597, and α2841D. Densitometry was performed using a Bio-Rad imaging densitometer (model GS-700) employing QuantityOne software (Bio-Rad). GAPDH, glyceraldehyde-3-phosphate dehydrogenase. (C) Northern analysis of total RNA from PF 29-13 cells and TbHK2-deficient cells. Total RNA (10 μg) was purified and electrophoresed in a formaldehyde–1.5% agarose gel. rRNA levels were estimated by ethidium bromide staining to ensure equal loading of RNAs. Densitometry was performed as described above.

TbHK2 localizes to glycosomes. To explore cellular localization, TbHK2 was expressed as a GFP fusion in *T. brucei*.

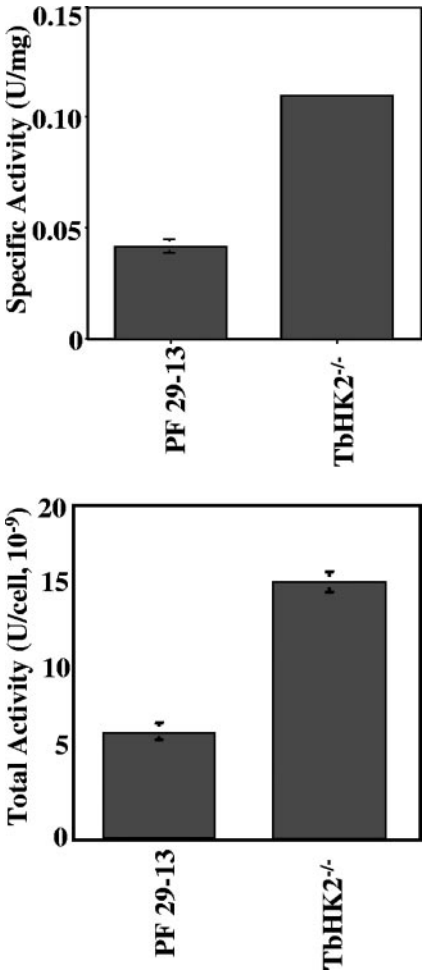

FIG. 4. Hexokinase activity in TbHK2 knockout cells. Parental (PF 29-13) and TbHK2$^{-/-}$ cells were grown in SDM-79, and cellular HK activity in detergent lysates was assessed.

Following induction, PF 29-13 cells expressing TbHK2-GFP were stained with a mouse monoclonal antibody against GFP and a rabbit anti-*T. brucei* glycosomal antibody (2841D) (21) (Fig. 5A). Both antibodies yielded similar staining patterns, and the overlay suggested glycosomal localization of TbHK2-GFP (Fig. 5A). Cells expressing GFP alone were diffusely green, without a punctate distribution of the signal (data not shown). Using affinity-purified αTbHK2 antibody for localization, TbHK2 localized in a punctate cytoplasmic pattern similar to that seen with the antiglycosomal antibodies (21; data not shown). This staining was not present in equivalent exposures of TbHK2$^{-/-}$ cells, indicating that the pattern is specific for TbHK2.

Morphology and growth are altered in TbHK2$^{-/-}$ PF parasites. One of the first differences noted between parental cells and the TbHK2 knockout cells was a change in cell shape. To explore this, we initially scored 10,000 cells by flow cytometry and found that PF 29-13 cells have a mean forward scattering value (which is proportional to size) of 237.5, while TbHK2 knockout cells are larger, with a mean forward scattering value of 279.6. This increase in size led us to explore the cell morphology by microscopy (Fig. 5B) While the TbHK2$^{-/-}$ cells were elongated, they maintained detectable glycosomes, as determined by antibody staining.

In addition to their elongated shape, TbHK2$^{-/-}$ cells grew more slowly in SDM-79 than did PF 29-13 cells, with a mean doubling time of 22 ± 2.5 h (compared to 14 ± 3 h for PF 29-13 cells). The influence of growth conditions on cell division time was explored further by the growth of parasites in SDM-80, which allows for manipulation of the glucose concentration. In low-glucose SDM-80 (0.15 mM), TbHK2$^{-/-}$ cells doubled every 20.4 ± 3.4 h, while in SDM-80 supplemented with high glucose (10 mM), the doubling time was 22.8 ± 1.5 h. PF 29-13 growth was similar to that of TbHK2$^{-/-}$ cells (and retarded compared to PF 29-13 growth in SDM-79, which is a more nutrient-rich medium), with doubling times of 19.5 ± 2 and 23.3 ± 1.7 h in low and high glucose, respectively. Additionally, TbHK2$^{-/-}$ cells maintained their elongated phenotype in both types of SDM-80.

Recombinant TbHK1 has hexokinase activity in vitro. Why does *T. brucei* harbor two nearly identical HK genes? We initially considered three possible explanations. First, the two proteins could be expressed in different life stages of the parasite, but given the recent purification and identification of both TbHKs from PF and BSF parasites (4), this scenario has been ruled out. Second, it is formally possible that the two proteins function in different subcellular compartments, even though both proteins contain identical PTS-2 glycosomal signal sequences in their N termini. The purification of both proteins from glycosome fractions (4), the characterization of active enzyme in glycosome preparations (15), and our glycosome localization of both endogenous TbHK2 and TbHK2 fused to GFP (Fig. 4) further argue against this possibility. Lastly, the proteins may have different kinetic properties, explaining the presence of two isoforms.

To consider the possibility that the two proteins use different

TABLE 1. Kinetic characterization of rTbHKs

Protein	Apparent K_m (mM)[a]				
	Glucose	ATP	Mannose	Fructose	$MgCl_2$
rTbHK1	0.09 ± 0.02	0.28 ± 0.1	0.03 ± 0.01	0.35 ± 0.3	0.92 ± 0.21
rTbHK2	ND	ND	ND	ND	ND
rTbHK1C2	ND	ND	ND	ND	ND
rTbHK2C1	0.07 ± 0.006	0.44 ± 0.11	0.05 ± 0.01	NA	0.58 ± 0.2
rTbHK1(N469D)	ND	ND	ND	ND	ND
Yeast Hxk	0.18 ± 0.1	0.25 ± 0.04	NA	NA	2.2 ± 0.42

[a] Data are means ± standard deviations. ND, not determined, as activity was not detected; NA, not assayed.

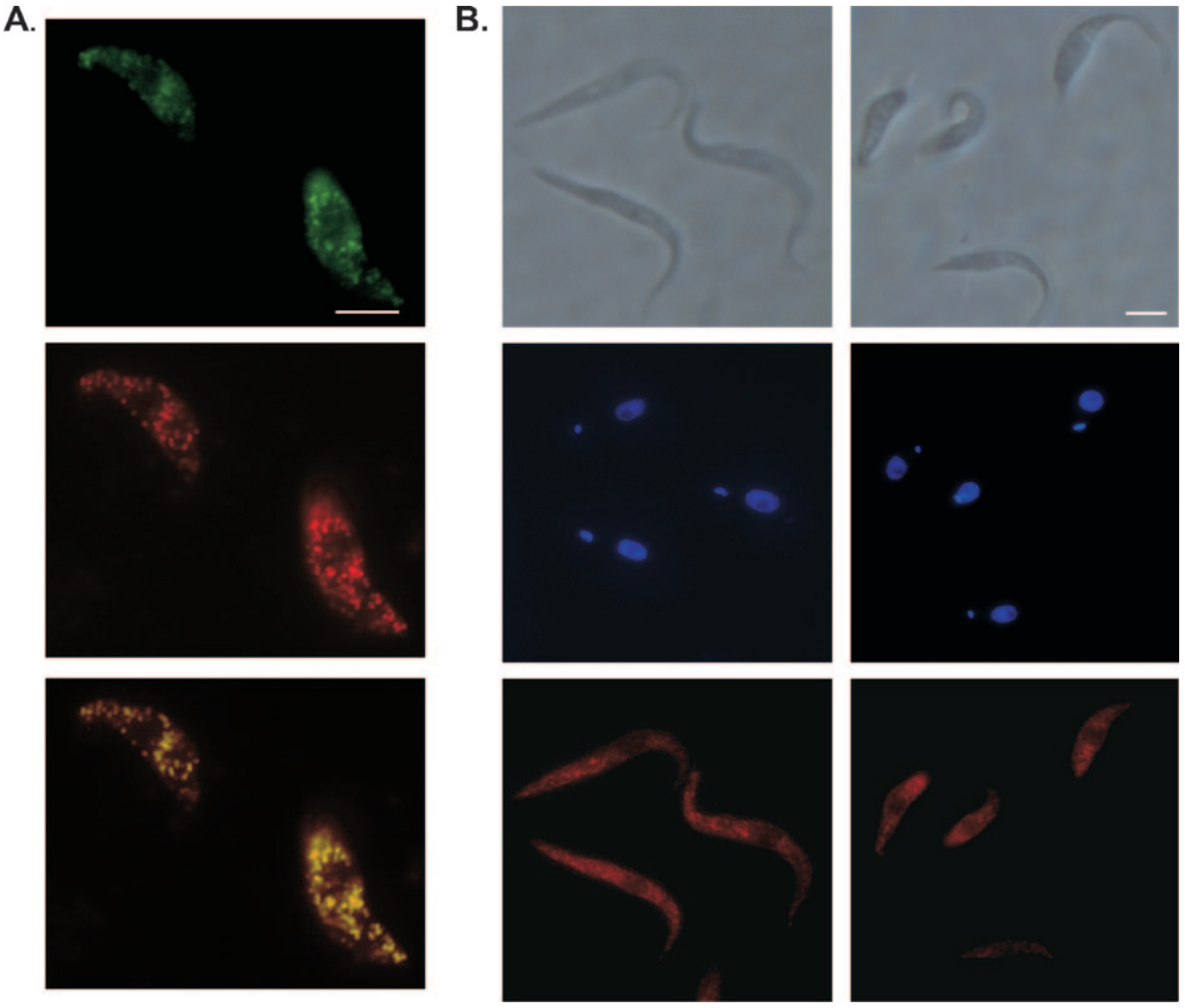

FIG. 5. Localization of TbHK2 by microscopy. (A) *T. brucei* cells expressing TbHK2-GFP from pLew111(2T7)GFPβ were fixed and stained with a mouse monoclonal antibody against GFP (top panel) and rabbit polyclonal 2841D antibodies against glycosomal proteins (center panel), and the images were overlaid (bottom panel). (B) Fixed parental PF 29-13 or knockout (TbHK2$^{-/-}$) parasites were stained with antiglycosomal antibodies (polyclonal 2841D antibodies). Bar = 10 μm.

substrates, we expressed both as recombinant proteins in *E. coli*. Soluble rTbHK1 and rTbHK2 were purified to ~95% homogeneity (as determined by Coomassie staining of an SDS-PAGE gel) (Fig. 6B) and assayed to explore their substrate selectivities and determine their kinetic parameters. Recombinant TbHK1 behaved much like other HKs, with apparent K_m values for glucose and ATP (0.09 ± 0.02 mM and 0.28 ± 0.1 mM, respectively) similar to those of yeast Hxk (0.18 ± 0.1 mM and 0.25 ± 0.04 mM, respectively) (Table 1). The rTbHK1 k_{cat} value was 2.9×10^4 min^{-1}, similar to that reported for a recently characterized *Trypanosoma cruzi* HK (6.8×10^4 min^{-1}) (2). While UTP was a substrate for rTbHK1 (apparent K_m, 0.15 ± 0.07 mM), activity was not detected with GTP, CTP, or ITP. Using UTP in the assay instead of ATP yielded a substantially reduced catalytic efficiency value of 2.4×10^3 min^{-1}.

In vitro, rTbHK1 was not limited to using glucose as a substrate. The enzyme phosphorylated mannose, fructose, 2-deoxyglucose, and glucosamine, with apparent K_m values of 0.03 ± 0.01 mM, 0.35 ± 0.35 mM, 0.11 ± 0.05 mM, and 0.23 ± 0.04 mM, respectively. G6-P, the product of HKs, did not inhibit rTbHK1 up to concentrations of 50 mM. Recombinant TbHK1 had an affinity for $MgCl_2$ (apparent K_m, 0.92 ± 0.21 mM) similar to that of yeast Hxk (2.2 ± 0.42 mM). When $CaCl_2$ was included in the standard assay in place of $MgCl_2$, neither rTbHK1 nor yeast Hxk was active.

In other HKs, residues that are orthologous to TbHK G^{93} and S^{161} are important for ATP binding and phosphoryl binding, respectively (10, 17). In *Arabidopsis*, an HK mutated at these positions is catalytically inactive but still competent for functioning in glucose sensing (17). To determine whether these residues are also important for TbHK1 activity, we generated site-directed mutants of TbHK1, namely, rTbHK1(G93D) and rTbHK1 (S161A). Both enzymes were soluble and inactive.

TbHK1 is inhibited by fatty acids but not by acyl-CoAs. Long-chain fatty acids (C_{14} to C_{20}) have been shown to inhibit mammalian HKs (23). To explore the impact of fatty acids on TbHK1 activity, rTbHK1 and yeast Hxk were incubated with

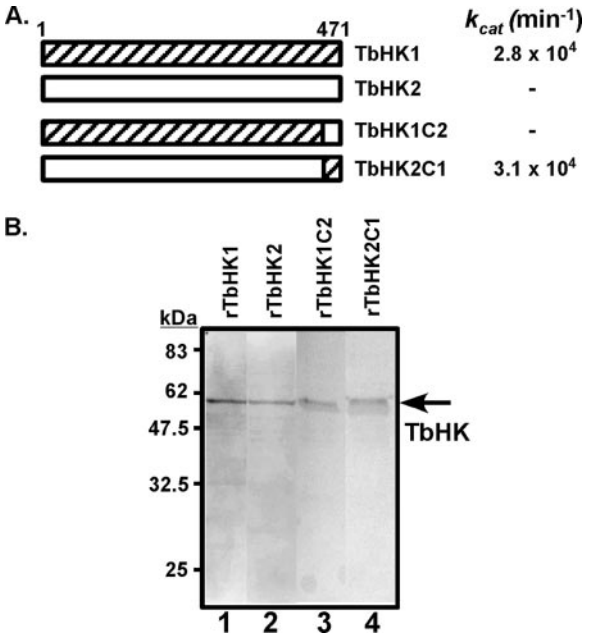

FIG. 6. Production of recombinant TbHK1 and -2 C-terminal mutants. (A) Schematic of C-terminal mutants and their HK catalytic rates. (B) SDS-PAGE analysis of the purification of histidine-tagged recombinant TbHKs. Lane 1, rTbHK1; lane 2, rTbHK2; lane 3, rTbHK1C2; lane 4, rTbHK2C1. Purified proteins (2 μg) were resolved by 12% SDS-PAGE and visualized by Coomassie staining.

saturated fatty acids with chain lengths from C_{10} to C_{18} and assayed for HK activity. While all fatty acids inhibited rTbHK1 at concentrations below their critical micelle concentrations (CMCs) (24), the most potent inhibition was observed with the medium-length fatty acids laurate (C_{12}), myristate (C_{14}), and palmitate (C_{16}) (50% inhibitory concentrations [IC_{50}s], 75.8, 78.4, and 62.4 μM, respectively) (Table 2). Inhibition observed with decanoate and stearate was weak, with IC_{50}s of >150 μM. Inhibition of TbHK1 by myristyl-coenzyme A (myristyl-CoA) or lauroyl-CoA was not observed at concentrations below the CMCs of these acyl-CoAs. Because of possible nonspecific detergent effects, concentrations above the CMCs were not tested. The control protein, yeast Hxk, was not inhibited by any of the fatty acids or acyl-CoAs tested.

rTbHK2 is inactive due to the influence of its C-terminal tail. Several observations led us to hypothesize that TbHK2 would be catalytically active in vitro, possibly with substrate or kinetic properties different from those of TbHK1. Firstly, TbHK1 and -2 are 98% identical. Secondly, 7 of the 10 amino acid differences cluster in the C-terminal 18 amino acids, a region that may not be essential for activity, as mutant yeast Hxk2 lacking the C terminus is still active (14). Lastly, TbHK1 and -2 share 61 of the 66 amino acids conserved in other HKs, as determined by Consurf analysis. The amino acid residues that diverge from those of other HKs are conserved between TbHK1 and -2.

We were surprised to find that while rTbHK1 behaved enzymatically like other HKs, rTbHK2 lacked detectable enzymatic activity. Assays including alternative hexoses as potential substrates (including mannose, fructose, 2-deoxyglucose, and glucosamine) with either $MgCl_2$ or $CaCl_2$ did not yield detectable activity. Additionally, ITP, CTP, GTP, UTP, PP_i, and ADP did not activate rTbHK2. We cannot rule out that rTbHK2, while being soluble, failed to fold properly. It should be noted that a comparison of rTbHK2 produced in bacteria with tagged TbHK2 expressed in *T. brucei* was not pursued because TbHKs are hexamers (15). These multimers could be a mixture of TbHK1 and -2, so purified TbHK2 may be "contaminated" with TbHK1.

The observation that rTbHK1 is active in vitro while rTbHK2 lacks detectable HK activity was surprising given the limited sequence differences between the proteins. Since 7 of the 10 amino acid differences between TbHK1 and TbHK2 are within the C-terminal tail, the C-terminal domains were exchanged to assess their impact on enzyme activity (Fig. 6A). TbHK1C2, which consists of the N terminus of TbHK1 fused with the TbHK2 C terminus, was inactive, while TbHK2C1 (TbHK2 with the C terminus of TbHK1) had activity similar to that of TbHK1 (Table 1). TbHK2 lacking the C-terminal 18 residues was soluble and inactive. We were unsuccessful in our attempts to express TbHK1 without the C-terminal 18 residues (or greater portions of the C terminus).

Amino acid differences between TbHK1 and TbHK2 cluster in a region adjacent to the interdomain cleft. TbHK1 and TbHK2 were modeled against yeast hexokinase PII, using DS Modeler (Fig. 7). This model revealed that the C-terminal tail resides near the interdomain cleft that is responsible for subunit movement after substrate binding (Fig. 7). Additional modeling against other hexokinases, including the *Schistosoma mansoni* HK (PDB code 1bdg) used in the original modeling of TbHK (which is now recognized as TbHK1) (28), confirmed the interdomain cleft localization of the tail.

In yeast, active-site residues, including the catalytic base Asp^{211} as well as Asn^{237}, Glu^{269}, and Glu^{302} (residues involved in glucose binding), are predicted to reside in an interdomain cleft (12). In addition to being part of the active site of the enzyme, the cleft acts as a hinge that allows a conformational change to take place upon substrate binding. Upon binding of glucose, the enzyme changes conformation, orienting residues required for catalysis within hydrogen bonding distance of the bound glucose molecule (12). The majority of the differences between TbHK1 and TbHK2 cluster in a small region near the putative active-site cleft in the hinge region. The three other amino acids that differ between TbHK1 and TbHK2 (residues 217, 219, and 267) also map to this interdomain region.

Many of the residues that differ in the tails of TbHK1 and -2 have side chains that are found on the same face of the α-helix (Fig. 7B). This positioning suggests that the interactions of the tail with the surrounding polypeptide could influence the global structure of the enzyme. Interestingly, the catalytic base Asp^{214} is positioned differently in the TbHK1 and TbHK2 models (Fig. 7C).

TABLE 2. Fatty acid inhibition of rTbHK1

Enzyme	IC_{50} (μM) of fatty acid[a]				
	C_{10}	C_{12}	C_{14}	C_{16}	C_{18}
rTbHK1	150	75.8	78.4	62.4	128.9
Yeast Hxk	ND	ND	ND	ND	ND

[a] ND, no inhibition observed, up to 150 μM fatty acid.

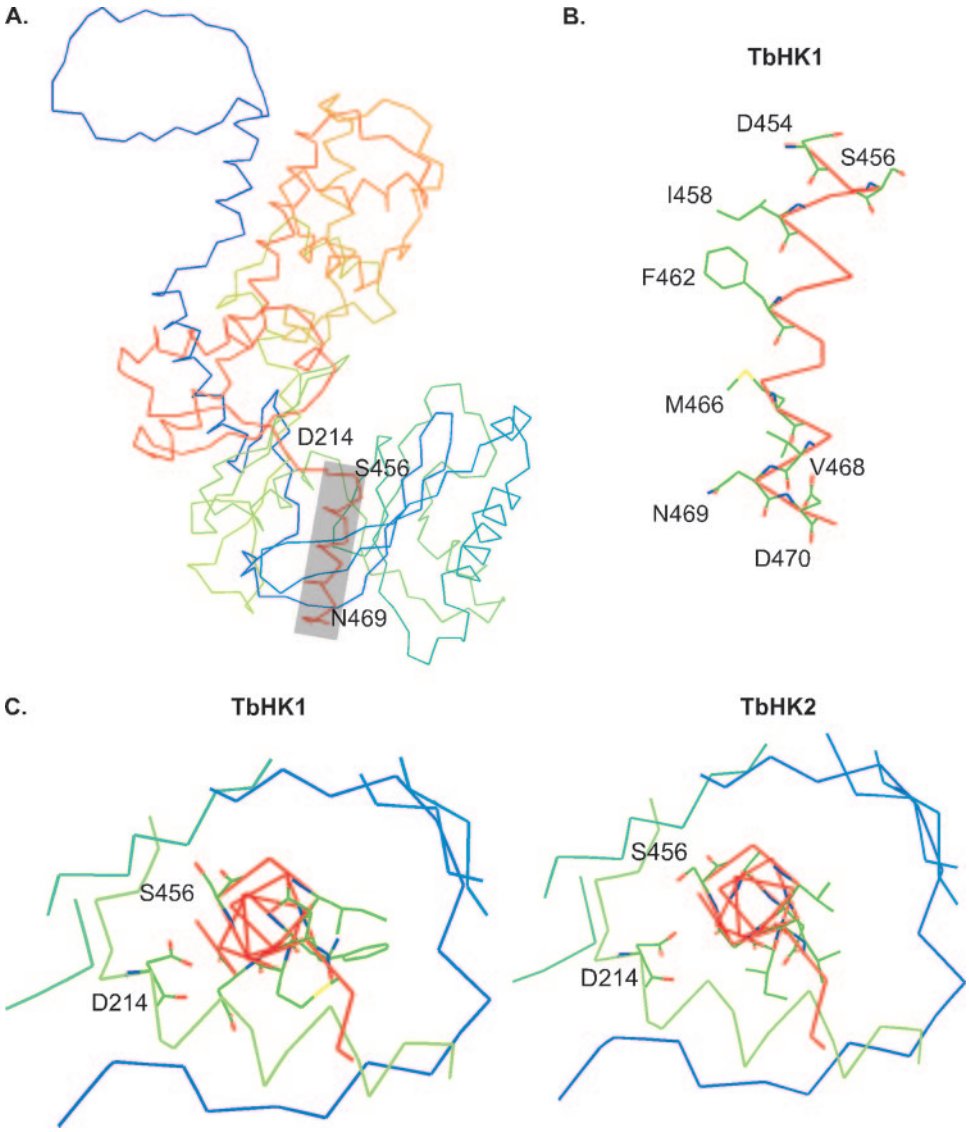

FIG. 7. Modeling of TbHKs. (A) DS Modeler-generated structure of TbHK1, using yeast hexokinase PII as the template. The boxed region corresponds to the location of the C-terminal 18 amino acids. D214 is the catalytic base, while S456 is an invariant residue in both TbHK1 and -2. (B) C-terminal tail of TbHK1. (C) Comparison of the influences of the C-terminal tails of TbHK1 and -2 on the positioning of D214. Note that the N-terminal signal sequences are unstructured in this model.

The altered positioning of the invariant Ser^{456} suggests that the overall tail conformations are different enough to alter the interaction of tail residues with the active site. To explore this possibility, site-directed mutagenesis was used to mutate TbHK1 Asn^{469} to Asp^{469} (the residue found in TbHK2) to yield TbHK1(N469D). This alteration, which is at the distal end of the tail, inactivates TbHK1 (Table 1). Modeling TbHK1(N469D) on yeast HK revealed that the catalytic base Asp^{214} and Ser^{456} are positioned more like the case in TbHK2 (not shown). These observations suggest that tail residues, even those removed from the active site, can influence the positioning of the helix relative to the active site.

The C-terminal ends of HKs tend to be the least-conserved region of the proteins, leading us to be cautious about the modeling of our C-terminal tail on other HKs. Others have modeled TbHK (now recognized to be TbHK1) on *S. mansoni* HK to assess inhibitor binding (28). Using a similar approach (with the last four residues excluded from the analysis, as was done in the original modeling on *S. mansoni* HK) (28), modeling revealed that the C-terminal 12 residues map to the hinge region of the enzyme, as found when yeast HK was used as the template.

DISCUSSION

T. brucei expresses two 98% identical polypeptides identified by homology searches as hexokinases in both PF and BSF life stages. To initiate studies on the role of these two proteins in the biology of the parasite, we generated TbHK2 knockout cells and explored the enzymology of the two gene products in

vitro. Our data suggest that TbHK2 is primarily a glycosomal protein that lacks detectable HK activity in vitro. However, parasites lacking TbHK2 have altered morphology, retarded growth, and increased cellular HK activity, suggesting that the protein serves a function in vivo distinct from that of TbHK1.

The genes for TbHK1 and TbHK2 are arranged in tandem on chromosome 10. Similarly arranged HK genes (or nearly identical duplicate HKs) are found in other medically important related kinetoplastid parasites. *T. b. gambiense* has genes in tandem on chromosome 10 that encode homologs of TbHK1 and TbHK2. *Leishmania major* has a pair of putative HK genes, which are 62% identical to the TbHK genes, located in tandem on chromosome 21 (LmjF21.0250 and LmjF21.0240). These genes encode nearly identical polypeptides (with a single amino acid difference between the two predicted polypeptides). The *T. cruzi* genome also encodes two highly related HKs (Tc00.1047053510121.20 and Tc00.1047053508951.20 [98.9% identical]), which are 67% identical to the TbHKs. Their chromosomal arrangement is unknown.

Multiple HK genes are not unique to kinetoplastid parasites. In *S. cerevisiae*, two highly related (75% identical at the amino acid level) HK genes, *hxk1* and *hxk2*, reside on chromosomes 6 and 7, respectively. Mammals also have multiple HKs, with three ~100-kDa isoforms (types I, II, and III) consisting of two monomer-like HKs fused together (which are likely the result of duplication and fusion of an ancestral HK) (3). The monomer-like HK domains are very similar to one another and to HKs found in yeast, *S. mansoni*, and *T. brucei* (29). Interestingly, the N-terminal monomer-like domains of the type I and III isoforms are enzymatically inactive, while the C-terminal domains house the catalytic activity. The inactive domains serve to regulate the function of the enzyme by binding G6-P. While the TbHK1 gene is not inhibited by its product, it is tempting to speculate that TbHK2, like the inactive N-terminal domains of type I and III HKs, regulates TbHK1, perhaps by binding to a regulatory molecule (currently unknown) which then triggers an interaction with TbHK1 that leads to altered enzyme activity.

Authentic HK activity from *T. brucei* likely consists of a multimer of TbHK1 and -2, as the original activity was purified with a molecular mass consistent with that of a hexameric complex. The multimer composition can alter HK activity. In yeast, HK dimerization is modulated by phosphorylation of Ser^{14}, with increased phosphorylation occurring as environmental glucose levels fall (25). This results in dissociation of the dimeric enzyme and an increase in enzyme affinity for glucose (1, 8). If TbHK2 is involved in the regulation of TbHK1, then the parasite could modulate the composition of the hexamer in order to respond to changes in glucose availability.

In addition to potential regulation by TbHK2, TbHK1 may be regulated by fatty acids found in the glycosome, the organelle in which the enzyme resides. Free fatty acids have been shown to inhibit mammalian cardiac hexokinase (23), and they are likely available in the glycosome, as a *T. brucei* acyl-CoA synthetase, the enzyme that converts fatty acids to acyl-CoAs, has been localized to this organelle (D. Jiang and P. Englund, personal communication). In support of the possibility of regulation by fatty acids, recombinant TbHK1 is inhibited by free fatty acids but not by acyl-CoA derivatives of the same fatty acids. Note, however, that partially pure HK from *Trypanosoma cruzi* is not inhibited by fatty acids but, rather, is inactivated by acyl-CoAs (7).

To study the function of TbHK1 and -2 in *T. brucei*, we attempted to knock out each gene. To date, we have been unable to generate homozygous null TbHK1 parasites, with the heterozygous null parasites displaying a severe growth phenotype (data not shown). Since recombinant TbHK1 has activity similar to that of other glycolytic HKs, the cellular phenotype could be due to a metabolic deficiency that results from haploinsufficiency.

Ablation of TbHK2 also leads to several phenotypes, including a retarded growth rate and altered cellular morphology. It is formally possible that rTbHK2 lacks a posttranslational modification required for activity. Yeast Hxk2, for example, is phosphorylated on Ser^{158} when the enzyme is incubated with the nonphosphorylatable substrate xylose, and the modification inhibits the enzyme (6, 9). Other sites of phosphorylation, including Ser^{14}, can alter yeast Hxk2 multimerization in vitro, which can ultimately change the catalytic properties of the enzyme (1, 8).

TbHK1 and TbHK2 harbor distinct C-terminal sequences, with the last 18 amino acids containing 7 of the 10 amino acid differences between the proteins. Comparison of the C-terminal 18 residues of TbHK2 with the C termini of HKs from other kinetoplastid organisms revealed that TbHK2 has a unique tail (Fig. 1). At five positions, TbHK2 has an amino acid that is not found in any of the other kinetoplastid HKs. However, most of the residues in the TbHK1 tail are conserved among the kinetoplastid HK C-terminal tails, with the lone exception of Met^{466}.

The observation that rTbHK1 is active while rTbHK2 is not suggests that the C terminus may regulate activity. Modeling the protein structures on that of yeast Hxk2 indicated that the differences lie within a cleft that separates the large and small domains of the enzyme. This cleft contains several active-site residues, including amino acids that are responsible for glucose binding as well as the general catalytic base (12). In addition to being part of the active site of the enzyme, the cleft is important for the conformational changes that take place upon substrate binding. In the absence of glucose, the enzyme is found in an "open" configuration, but upon binding of glucose, the two domains are brought closer together, drawing residues required for catalysis within hydrogen bonding distance of the bound glucose (12).

It is possible that the unique C-terminal sequence of TbHK2 alters the positioning of the catalytic base or prevents conformational changes required for enzyme activity. In support of these ideas, replacing the C terminus of TbHK1 with the corresponding amino acids from TbHK2 resulted in an inactive protein. Changes in the C-terminal tail of yeast Hxk2 are apparently more tolerated, as mutant Hxk2 lacking the 10 C-terminal residues remains active (but does exhibit differences in kinetics, with a threefold increase in the K_m for fructose and a marked decrease in glucose phosphorylation activity) (14).

What do these nearly identical polypeptides do for *T. brucei*? The differences in phenotypes and in vitro activity suggest distinct functions for TbHK1 and -2, with TbHK1 perhaps serving as the primary metabolic enzyme while TbHK2 per-

forms a regulatory or signaling role. There is precedence for multiple similar HKs that serve different functions, although the proteins are less similar than the nearly identical ones from *T. brucei*. For example, yeast Hxk1 and Hxk2 and yeast glucokinase can all catalyze the phosphorylation of glucose. Yeast Hxk2 has other functions, however, including participating in the glucose-induced repression pathway by moving to the nucleus to transmit the repression response (22). *Arabidopsis thaliana* hexokinase 1 (AtHXK1) has been shown to play a role in signal transduction, even in the absence of catalytic activity (17). Lastly, a *Leishmania* HK involved in hemoglobin endocytosis has been found localized to the flagellar pocket (11). These observations suggest that TbHK2 may function in pathways distinct from glucose phosphorylation, providing an area of ongoing research.

ACKNOWLEDGMENTS

We thank Kojo Mensa-Wilmot, Paul T. Englund, and Kimberly Paul for their helpful comments on the manuscript. We also thank Harry Kurtz for the use of his microscope.

Z.Y. was supported by a grant from The Foundation of Kunming Medical College for Science and Advanced Academic Teachers, by The National Natural Science Foundation of China (grant 30560022), and by the China Scholarship Council (grant 2003853016).

REFERENCES

1. **Behlke, J., K. Heidrich, M. Naumann, E. C. Muller, A. Otto, R. Reuter, and T. Kriegel.** 1998. Hexokinase 2 from *Saccharomyces cerevisiae*: regulation of oligomeric structure by in vivo phosphorylation at serine-14. Biochemistry **37:**11989–11995.
2. **Caceres, A. J., R. Portillo, H. Acosta, D. Rosales, W. Quinones, L. Avilan, L. Salazar, M. Dubourdieu, P. A. Michels, and J. L. Concepcion.** 2003. Molecular and biochemical characterization of hexokinase from *Trypanosoma cruzi*. Mol. Biochem. Parasitol. **126:**251–262.
3. **Cardenas, M. L., A. Cornish-Bowden, and T. Ureta.** 1998. Evolution and regulatory role of the hexokinases. Biochim. Biophys. Acta **1401:**242–264.
4. **Colasante, C., M. Ellis, T. Ruppert, and F. Voncken.** 2006. Comparative proteomics of glycosomes from bloodstream form and procyclic culture form *Trypanosoma brucei* brucei. Proteomics **6:**3275–3293.
5. **Drew, M. E., J. C. Morris, Z. Wang, L. Wells, M. Sanchez, S. M. Landfear, and P. T. Englund.** 2003. The adenosine analog tubercidin inhibits glycolysis in *Trypanosoma brucei* as revealed by an RNA interference library. J. Biol. Chem. **278:**46596–46600.
6. **Fernandez, R., P. Herrero, E. Fernandez, T. Fernandez, Y. S. Lopez-Boado, and F. Moreno.** 1988. Autophosphorylation of yeast hexokinase PII. J. Gen. Microbiol. **134:**2493–2498.
7. **Garcia de Lema, M., G. Lucchesi, G. Racagni, and E. E. Machado-Domenech.** 2001. Changes in enzymatic activities involved in glucose metabolism by acyl-CoAs in *Trypanosoma cruzi*. Can. J. Microbiol. **47:**49–54.
8. **Golbik, R., M. Naumann, A. Otto, E. Muller, J. Behlke, R. Reuter, G. Hubner, and T. M. Kriegel.** 2001. Regulation of phosphotransferase activity of hexokinase 2 from *Saccharomyces cerevisiae* by modification at serine-14. Biochemistry **40:**1083–1090.
9. **Heidrich, K., A. Otto, J. Behlke, J. Rush, K. W. Wenzel, and T. Kriegel.** 1997. Autophosphorylation-inactivation site of hexokinase 2 in *Saccharomyces cerevisiae*. Biochemistry **36:**1960–1964.
10. **Kraakman, L. S., J. Winderickx, J. M. Thevelein, and J. H. De Winde.** 1999. Structure-function analysis of yeast hexokinase: structural requirements for triggering cAMP signalling and catabolite repression. Biochem. J. **343:**159–168.
11. **Krishnamurthy, G., R. Vikram, S. B. Singh, N. Patel, S. Agarwal, G. Mukhopadhyay, S. K. Basu, and A. Mukhopadhyay.** 2005. Hemoglobin receptor in *Leishmania* is a hexokinase located in the flagellar pocket. J. Biol. Chem. **280:**5884–5891.
12. **Kuser, P. R., S. Krauchenco, O. A. Antunes, and I. Polikarpov.** 2000. The high resolution crystal structure of yeast hexokinase PII with the correct primary sequence provides new insights into its mechanism of action. J. Biol. Chem. **275:**20814–20821.
13. **Lamour, N., L. Riviere, V. Coustou, G. H. Coombs, M. P. Barrett, and F. Bringaud.** 2005. Proline metabolism in procyclic *Trypanosoma brucei* is down-regulated in the presence of glucose. J. Biol. Chem. **280:**11902–11910.
14. **Mayordomo, I., and P. Sanz.** 2001. Hexokinase PII: structural analysis and glucose signalling in the yeast *Saccharomyces cerevisiae*. Yeast **18:**923–930.
15. **Misset, O., O. J. Bos, and F. R. Opperdoes.** 1986. Glycolytic enzymes of *Trypanosoma brucei*. Simultaneous purification, intraglycosomal concentrations and physical properties. Eur. J. Biochem. **157:**441–453.
16. **Misset, O., and F. R. Opperdoes.** 1984. Simultaneous purification of hexokinase, class-I fructose-bisphosphate aldolase, triosephosphate isomerase and phosphoglycerate kinase from *Trypanosoma brucei*. Eur. J. Biochem. **144:**475–483.
17. **Moore, B., L. Zhou, F. Rolland, Q. Hall, W. H. Cheng, Y. X. Liu, I. Hwang, T. Jones, and J. Sheen.** 2003. Role of the *Arabidopsis* glucose sensor HXK1 in nutrient, light, and hormonal signaling. Science **300:**332–336.
18. **Morris, J. C., Z. Wang, M. E. Drew, and P. T. Englund.** 2002. Glycolysis modulates trypanosome glycoprotein expression as revealed by an RNAi library. EMBO J. **21:**4429–4438.
19. **Nwagwu, M., and F. R. Opperdoes.** 1982. Regulation of glycolysis in *Trypanosoma brucei*: hexokinase and phosphofructokinase activity. Acta Trop. **39:**61–72.
20. **Palma, F., S. Longhi, D. Agostini, and V. Stocchi.** 2001. One-step purification of a fully active hexahistidine-tagged human hexokinase type I overexpressed in *Escherichia coli*. Protein Expr. Purif. **22:**38–44.
21. **Parker, H. L., T. Hill, K. Alexander, N. B. Murphy, W. R. Fish, and M. Parsons.** 1995. Three genes and two isozymes: gene conversion and the compartmentalization and expression of the phosphoglycerate kinases of *Trypanosoma* (*Nannomonas*) *congolense*. Mol. Biochem. Parasitol. **69:**269–279.
22. **Rodriguez, A., T. De La Cera, P. Herrero, and F. Moreno.** 2001. The hexokinase 2 protein regulates the expression of the GLK1, HXK1 and HXK2 genes of *Saccharomyces cerevisiae*. Biochem. J. **355:**625–631.
23. **Stewart, J. M., and J. A. Blakely.** 2000. Long chain fatty acids inhibit and medium chain fatty acids activate mammalian cardiac hexokinase. Biochim. Biophys. Acta **1484:**278–286.
24. **Tippett, P. S., and K. E. Neet.** 1982. Specific inhibition of glucokinase by long chain acyl coenzymes A below the critical micelle concentration. J. Biol. Chem. **257:**12839–12845.
25. **Vojtek, A. B., and D. G. Fraenkel.** 1990. Phosphorylation of yeast hexokinases. Eur. J. Biochem. **190:**371–375.
26. **Wang, L., T. L. Kaduce, and A. A. Spector.** 1991. Myristic acid utilization and processing in BC3H1 muscle cells. J. Biol. Chem. **266:**13883–13890.
27. **Wang, Z., J. C. Morris, M. E. Drew, and P. T. Englund.** 2000. Inhibition of *Trypanosoma brucei* gene expression by RNA interference using an integratable vector with opposing T7 promoters. J. Biol. Chem. **275:**40174–40179.
28. **Willson, M., Y. H. Sanejouand, J. Perie, V. Hannaert, and F. Opperdoes.** 2002. Sequencing, modeling, and selective inhibition of *Trypanosoma brucei* hexokinase. Chem. Biol. **9:**839–847.
29. **Wilson, J. E.** 1997. An introduction to the isoenzymes of mammalian hexokinase types I-III. Biochem. Soc. Trans. **25:**103–107.
30. **Wirtz, E., S. Leal, C. Ochatt, and G. A. Cross.** 1999. A tightly regulated inducible expression system for conditional gene knock-outs and dominant-negative genetics in *Trypanosoma brucei*. Mol. Biochem. Parasitol. **99:**89–101.